Proc. Indian Acad. Sci. (Chem. Sci.), Vol. 97, Nos 3 & 4, October 1986, pp. 495–511.
© Printed in India.

Corrosion of austenitic stainless steels in aqueous environments[§]

J B GNANAMOORTHY
Materials Development Laboratory, Indira Gandhi Centre for Atomic Research, Kalpakkam 603 102, India

Abstract. Aqueous corrosion of austenitic stainless steels and their weldments has been reviewed, with particular reference to the results of the studies conducted at the Indira Gandhi Centre for Atomic Research at Kalpakkam. Different aspects of pitting and crevice corrosion, intergranular corrosion and stress corrosion cracking in stainless steels have been discussed. Since secondary phases present in these stainless steels have a significant influence on the corrosion behaviour of these steels, the methods of estimation of these secondary phases have also been discussed.

Keywords. Austenitic stainless steels; aqueous corrosion; pitting; crevice corrosion; stress corrosion cracking; sensitization; intergranular corrosion; secondary phases; carbides; delta-ferrite; sigma; chi-phase; weldments.

1. Introduction

Stainless steels are extensively used as materials of construction because of their good corrosion resistance, and in many applications problems due to corrosion do not arise. However, attempts to extend their use to more demanding technological applications has continued to generate interest in their corrosion resistance, often with a view to defining limits for their use. Austenitic stainless steels, which are the modifications of the classic 18% Cr-8% Ni iron based alloys and designated by the 300 series of the American Iron and Steel Institute (AISI), represent the largest category of stainless steels produced in the world. From among the austenitic steels type 316 stainless steel has been used as the material for fuel cladding as well as for most of the structural components of the sodium cooled fast breeder reactors. Various aspects of the corrosion behaviour of this stainless steel and other related alloys in aqueous environments have been extensively studied since 1975 in the Materials Development Laboratory of the Indira Gandhi Centre for Atomic Research at Kalpakkam. A review of these studies is presented here.

2. Pitting corrosion

Usually adequate allowance in the wall thickness of the component is made at the design stage to take into account the possible loss of material by uniform corrosion during its service life. A serious mode of attack of stainless steels is localized corrosion such as pitting, crevice corrosion, intergranular corrosion and stress corrosion cracking. Therefore, detailed studies are very essential for understanding and defining conditions under which a given alloy/environment system will undergo such a localized attack.

[§] Dedicated to Prof. K S G Doss on his eightieth birthday.

It is well-recognized that pitting corrosion of metals takes place only at potentials higher than a critical value for each alloy/environment system (Gnanamoorthy and Balachandra 1973). During the evaluation of the critical potential for AISI type 316 ss in 0·1 N H_2SO_4 containing 0·5 N Cl^- ions by the potentiostatic method (Dayal and Gnanamoorthy 1980b), it was observed that before stable and self-propagating pits are formed, unstable pits are nucleated and repassivated. The initiation of unstable pits is indicated by the rise of the current in the form of either flicks or a gradual increase and then a sudden decrease before a steady rise of current at the stable pitting potential during anodic polarization. The incubation periods for nucleation of unstable and stable pitting were determined at various constant potentials for a maximum exposure period of 24 hr. The plots of inverse of incubation time (i.e., rate of initiation of pits) vs. potential were found to be linear for both unstable and stable pitting (figure 1). Since the critical potential for the stable pitting (E_{sp}) and the critical potential for unstable pitting (E_{up}) are those potentials at which the rates of initiation of stable and unstable pits, respectively, are zero (i.e., incubation periods are infinite), they can be more accurately determined as the intercepts of these linear plots obtained by the least square method. The values of E_{sp} and E_{up} (+537 and +449 mV, respectively) thus determined were quite close to the ranges of values evaluated by the experiments.

Two more critical potentials, namely the instantaneous potential for unstable pits, E_{iup}, and the instantaneous potential for stable pits, E_{isp}, were also identified. At these critical potentials, the incubation periods for nucleation of unstable pits and stable pits respectively were zero, and pitting started instantaneously. The values of E_{iup} and E_{isp} could be determined accurately from the intercepts of the linear plots of potential vs. incubation time (figure 2). It was also shown that the pit nucleation potentials obtained by potentiodynamic as well as semi-potentiostatic experiments correspond to the nucleation of unstable pitting. The critical pit passivation potential, E_{pp}, defined as that potential more active

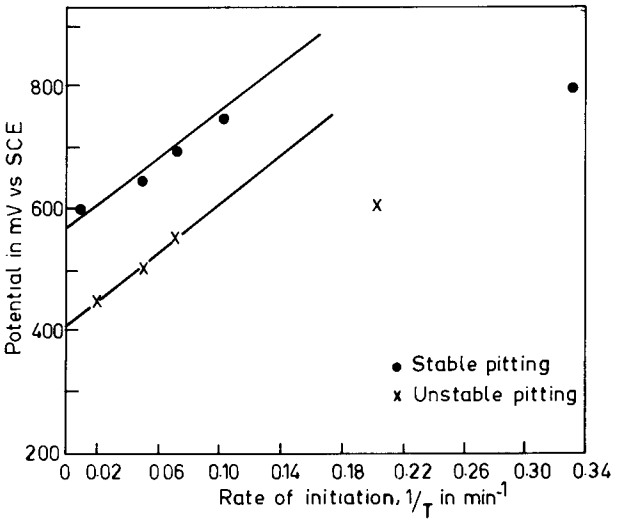

Figure 1. Plots of applied potential vs. rate of initiation of pits (i.e. inverse of incubation time) during stable and unstable pitting.

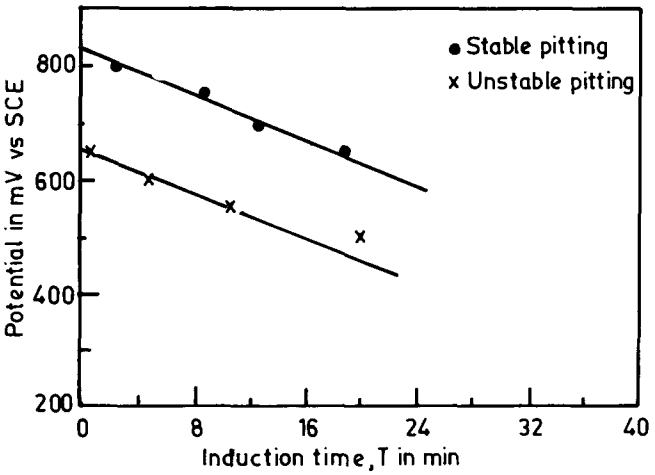

Figure 2. Plots of applied potential vs. induction time for stable and unstable pitting.

to which neither new pits can nucleate nor existing pits propagate, can be considered as a unique material property, provided that the value of E_{pp} is determined by universally standarized experimental conditions and the pit growth value limited to about 0·1 mA/cm^2 (Dayal and Gnanamoorthy 1979, 1980b).

The kinetics of pit growth has been generally observed to follow a relationship of the type $i = kt^b$ where i is the increase in the current density after a time t that has elapsed after the initiation of the pit. The value of the exponent b depends on a number of factors such as the alloy composition, applied potential, composition of the medium and pit density. In the case of unstable pits, the values of b at different potentials and chloride concentrations were found to vary randomly, indicating that they do not follow any regular kinetics. In the case of stable pit growth, at lower applied potentials and chloride concentrations two distinct values of b were found, indicating a change in kinetics after the initial growth of the pits. At higher applied potentials and chloride concentrations, a value close to 2 was obtained for b throughout the period of growth of the pit (figures 3 & 4). It was also observed that the pits initiated at the interface of the alloy and the inclusion, and that the morphology of the pit gradually changed from a regular to an irregular shape during different stages of the pit growth (Dayal and Gnanamoorthy 1979, 1982).

In general, the corrosion of a weld metal is known to be inferior to that of the base metal because of the inhomogeneous, dendritic microstructure produced in the former after welding. On prolonged exposure at high temperatures, the microstructure undergoes further changes due to precipitation of more secondary phases. Gill *et al* (1986a) have studied the pitting corrosion behaviour of weld deposit metal of type 316L ss after thermally ageing it at 773, 873 and 973 K for different durations of time ranging from 0·5 to 5000 h. They found that the pitting corrosion resistance of the weld metal decreases with ageing time at all the temperatures studied (figure 5). With the decrease in the pit nucleation potential there was a corresponding increase in the reactivation peak current density (figure 6). The delta-ferrite and sigma phases in the weld metal remained

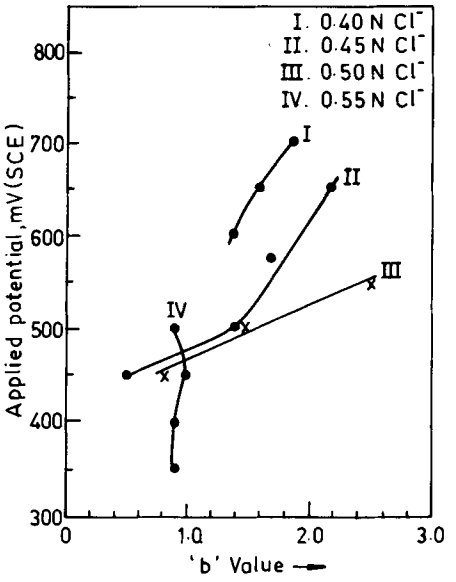

Figure 3. Variation of *b* value with respect to applied potential for different chloride ion concentrations during stable pit growth.

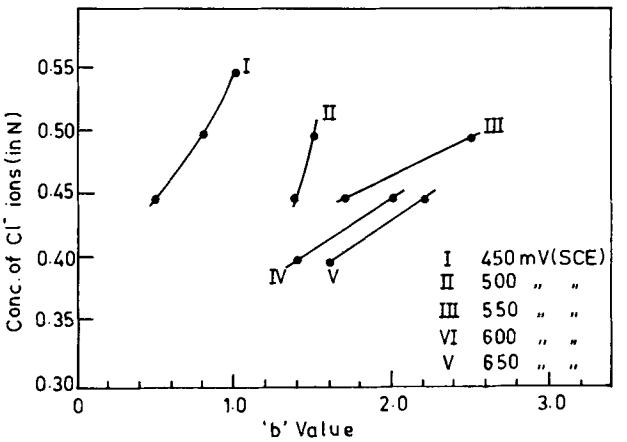

Figure 4. Variation of *b* value with respect to applied potential for different chloride ion concentrations during unstable pit growth.

unattacked during pit growth because of their relatively nobler electrochemical properties.

Recently it has been reported that the addition of small amounts of nitrogen to the weld metal as well as wrought metal improves their pitting corrosion and sensitization resistances and their mechanical properties. Kamachi Mudali *et al* (1986) have studied the role of nitrogen in improving the pitting corrosion resistance of weldments of 304 and 316 stainless steels. Weld metal samples with different levels of nitrogen were obtained by autogenous TIG welding process with

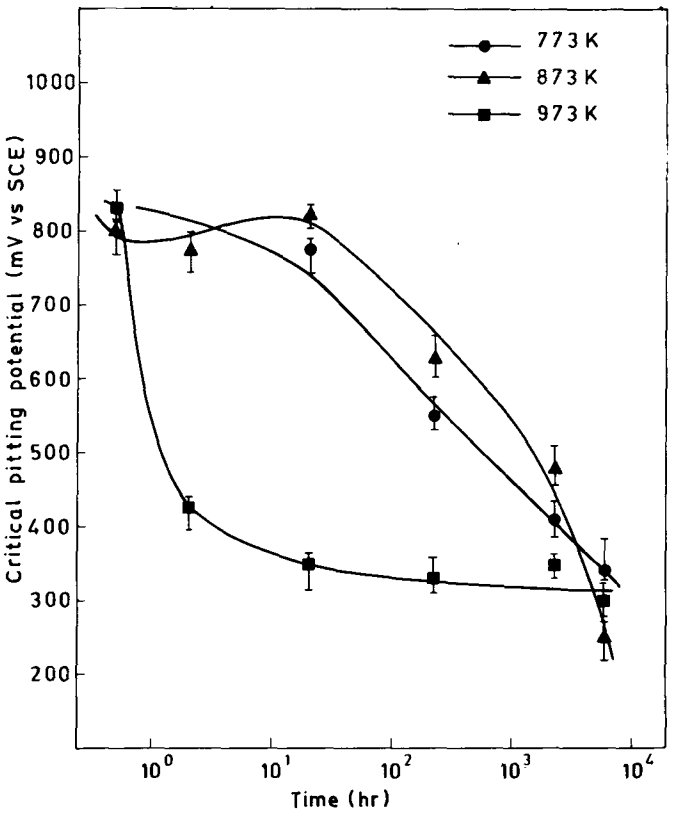

Figure 5. Variation in the critical pitting potential with ageing time at 773, 873 and 973 K.

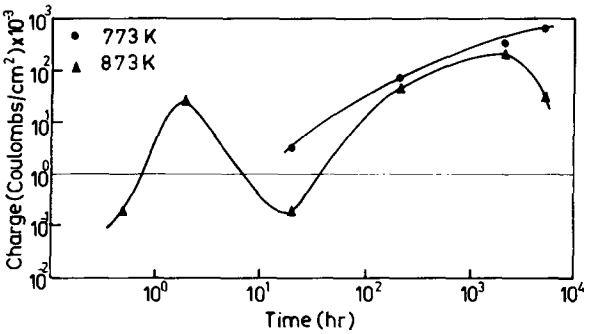

Figure 6. Change in the reactivation peak current density with ageing time at 773 and 873 K.

varying proportions of argon-nitrogen mixtures as the shielding gas. The nitrogen content in the weld metal was found to increase as the volume percent of nitrogen in the argon gas was increased (figure 7). While there was no delta-ferrite present in the weld metals of type 316 ss even at very low levels of nitrogen in the metal, delta-ferrite was absent in type 304 ss weld metal samples only when the concentration of nitrogen in the weld metal was very high (~1400 ppm).

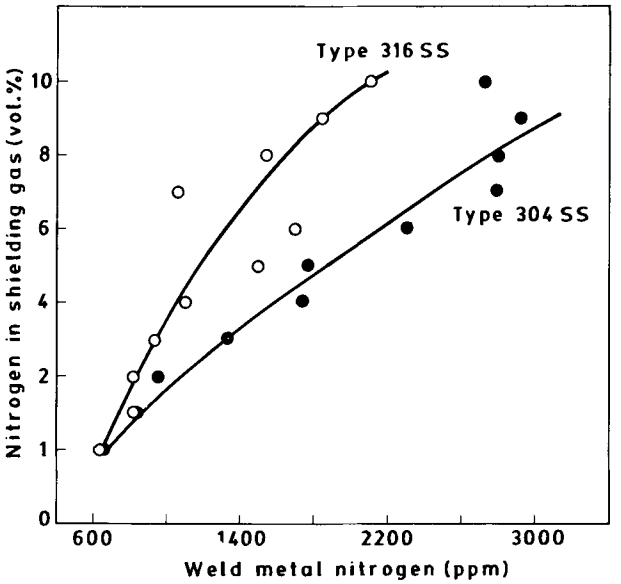

Figure 7. Nitrogen contents in weld metals of types 304 and 316 ss as a function of the volume percent of nitrogen gas mixed with shielding argon gas.

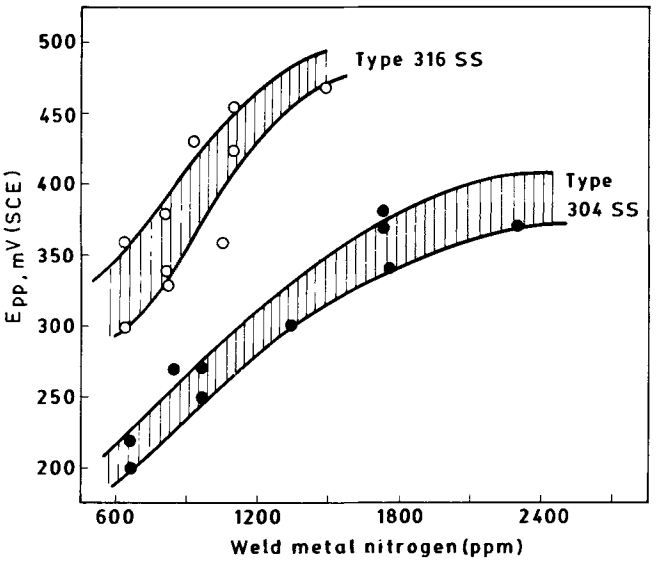

Figure 8. Critical pitting potentials of types 304 and 316 ss weld metals as a function of their nitrogen content.

Potentiodynamic anodic polarization studies in 0·5 M NaCl solution (deaerated by hydrogen) showed that weldments of both types of steel had increased resistance to pitting as the nitrogen content in the steel was increased (figure 8).

The specific role of nitrogen in improving the pitting corrosion resistance was studied by ESCA evaluation of the pitted samples. The passive film on the samples showed the absence of nitrogen and molybdenum; however, these elements were

found to be enriched at the metal/film interface. A 4 eV peak shift in the nitrogen found at the pit site indicated the presence of a nitrogen compound at the pit. This lent credence to the hypothesis of the dissolution of nitrogen to form NH_4^+ ions and subsequently other inhibiting compounds which repassivate the pit surface to improve the pitting corrosion resistance.

Examination of the pitted samples of type 316 ss weldments by scanning electron microscopy and optical microscopy showed that pits had initiated at triple points of austenite/austenite boundaries as well as at centres of the austenite grains. Triple points are the regions where the impurities or the minor alloying elements such as S and P segregate to the maximum extent during primary austenite solidification. The occurrence of pits at austenite centres could be due to the fact that these areas have the lowest concentrations of Cr and Mo compared to the grain boundary regions in the weld metal. In the case of type 304 ss weld metal samples, pits were found to initiate at austenite/delta-ferrite interfaces and grow into the austenite matrix leaving the Cr-rich delta-ferrite unattacked.

Based on the available results and observations, a generalized mechanism for pitting could be put forward:

1. At a potential more noble to a critical value, due to the presence of certain inhomogenities on the metal surface, passivity is momentarily destroyed by either penetration or adsorption of aggressive ions or by film breaking mechanisms.
2. The metal dissolution process produces M^{n+} ions inside the pit.
3. Due to the excess positive charge inside the pit, negative ions like Cl^- are attracted to attain electrical neutrality and thus the metal chloride (MCl_n) is formed.
4. Hydrolysis MCl_n generates a very low pH, and insoluble corrosion products are formed inside the localized area.
5. The highly acidic environment increases the dissolution rate further which attracts more Cl^- ions and the process becomes autocatalytic.
6. Besides the activating Cl^- ions, other non-activating ions such as OH^- and SO_4^{--} present in the bulk solution are also attracted to the local site. The autocatalytic process is retarded and the film is likely to be rendered stable again. Stable pitting takes place only if conditions are created at localized areas for autocatalytic process (like low pH, high Cl^- concentration etc.). Unstable pitting occurs when any of the conditions for autocatalytic process is not met, so that a pit could be repassivated.

3. Crevice corrosion

Another form of localized corrosion which is a major practical problem affecting stainless steels is crevice corrosion. This occurs in shielded areas of metal surfaces formed at the interfaces of pipe couplings, threaded or rivetted connections, gasket fittings, spot welded lap joints, porous welds, coiled or stacked sheets of metals etc. Extensive investigations have been carried out towards understanding the mechanism of crevice corrosion and a recent review by Dayal and Gnanamoorthy (1983b) describes in brief the results of these investigations. The unified mechanism for crevice corrosion, which is presently favoured, is described below:

Initially, the anodic dissolution ($M \rightarrow M^+ + e$) and cathodic reduction ($O_2 + 2H_2O + 4e \rightarrow 4OH^-$ in neutral solution) processes occur uniformly over the entire metal surface, including the crevice exterior. The oxygen in the shielded crevice area is consumed after some incubation period, but the decrease in cathodic reduction rate is negligible because of the small area involved. Consequently the corrosion of the metal inside and outside the crevice continues at the same rate. With cessation of the cathodic reactions producing hydroxide, the migration of negative ions (e.g. chlorides) into the crevice area is required to maintain charge balance. The resulting metal chloride hydrolyses to insoluble metal hydroxides and free acid. Both the chloride ions and low pH accelerate crevice corrosion in a manner similar to autocatalytic pitting, while the reduction reaction cathodically protects the exerior surface.

Initiation of crevice corrosion attack can be influenced by a number of factors such as the crevice geometry, alloy composition and its microstructure, bulk solution chemistry as well as physical characteristics such as temperature, velocity and volume. Dayal *et al* (1983a) have used a potentiodynamic polarization method for assessing the influence of these various factors on the crevice corrosion

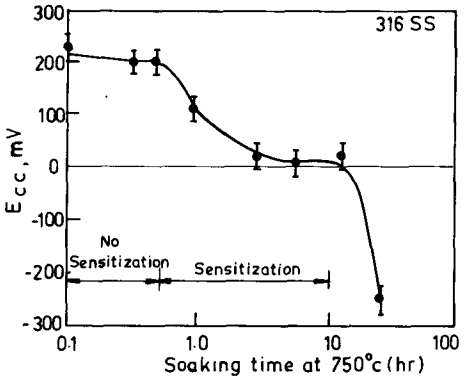

Figure 9. Relationship between critical crevice corrosion potential, E_{cc}, and soaking time (degree of sensitization).

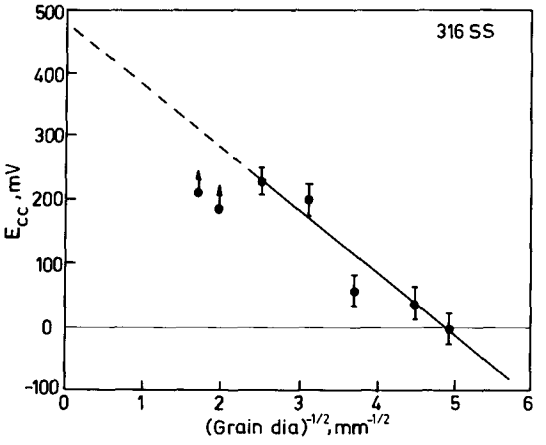

Figure 10. Relationship between E_{cc} and grain diameter.

resistance of austenitic stainless steels of types 304, 310 and 316 in 0·5 M NaCl solution. The critical crevice potential, E_{cc}, determined in these experiments was used as the index to the crevice corrosion resistance of a given system (a more active E_{cc} value indicating a higher susceptibility to crevice attack). Dayal and Gnanamoorthy (1984) observed that sensitized samples of type 316 ss in 0·5 M NaCl solution exhibit increased susceptibility to crevice corrosion and suffer intergranular attack inside the crevice (figure 9). They also found that the resistance to crevice corrosion decreases with decrease in the grain diameter (d) following a linear relationship between E_{cc} and $d^{-1/2}$ (figure 10). Investigations on cold worked stainless steels of types 304, 310 and 316 stainless steels indicated that E_{cc} decreases with cold work up to 5 to 15% and that further increase in cold work did not produce any further change in E_{cc} value. These effects were attributed to the increase in the number of defect sites and change in texture produced by cold work (Dayal *et al* 1984).

4. Sensitization and intergranular corrosion

When austenitic stainless steels are heated in the temperature range of 723 to 1123 K, the chromium present in them combines with carbon and precipitates at the grain boundaries as chromium-rich carbides such as $Cr_{23}C_6$. This carbide precipitation with the accompanying depletion of chromium in the vicinity of the grain boundaries is known as sensitization. The chromium concentration in the areas adjacent to the grain boundaries may fall below the minimum required value (about 12%) for maintaining passivity, if the component is heated for a sufficiently long time in this temperature range. When this happens the component is liable to undergo selective grain boundary attack during its service, resulting in intergranular corrosion. Optimum parameters for heat treatment to avoid sensitazation can be obtained from time-temperature-sensitization (TTS) diagrams for the required stainless steels. Dayal *et al* (1978) have established the TTS diagram for a modified type 316 stainless steel. The influence of different degrees of cold work (0 to 25% reduction in thickness by cold rolling) on the sensitization behaviour of type 316 ss has also been studied (Dayal *et al* 1981). The TTS diagrams for these cold worked steels showed that the temperature range increases as the cold work increased up to 10%. However, the time required for sensitization is reduced around the nose temperatures with increase in cold work up to 10%. At higher cold work levels, both the temperature range of sensitization and the time required for sensitization remain almost the same.

While the TTS diagram can be used for evaluating the sensitization time for any isothermal heat treatment, it cannot be used directly to determine the extent of sensitization when the material is continuously cooled through a range of temperatures. Dayal and Gnanamoorthy (1980a) have developed a method to predict the extent of sensitization in stainless steels during continuous cooling. The principle of this method is similar to that used for relating time-temperature-transformation behaviour on continuous cooling. Using this method the critical linear cooling rate to avoid sensitization can be calculated for a material whose TTS diagram is known. Dayal *et al* (1981) have shown that based on this method a continuous cooling sensitization (CCS) diagram can also be established from the isothermal TTS diagram and the different cooling curves.

5. Stress corrosion cracking

Many incidents of stress corrosion cracking in stainless steel components, especially in water cooled nuclear reactors, have been experienced throughout the world. Intergranular cracking has been widely reported in weld-sensitized regions. In many cases intergranular or transgranular cracking has been found in regions away from the welds as well as in components that were not welded. Such crackings have been attributed to the presence of chloride and oxygen in water. In view of the seriousness of the problems posed by stress corrosion cracking in critical reactor components, systematic investigations of the factors affecting the phenomenon have been carried out. Khatak and Gnanamoorthy (1979) have studied the stress corrosion cracking of type 304 ss in water containing zero to 50 ppm of oxygen and 10 and 50 ppm of chloride ions at 280°C with the C-ring specimens stressed to 70% and 100% of the yield strength of the alloy. The results showed that the specimens stressed to 70% yield strength and exposed to a solution containing no oxygen but 10 ppm of chloride ions did not undergo any cracking up to 340 days of exposure. However, under similar experimental conditions except for an increase in oxygen ion concentration (achieved by not adding hydrazine), the specimens had cracked after an exposure period of 225 days. When the chloride ion concentration was increased to 50 ppm the cracking time was reduced to 162 days. Similarly, any increase in the stress level or oxygen level further decreased the time to cracking. In all the cases the cracking was transgranular. Thus, it was shown that both chloride and oxygen levels in water need to be simultaneously controlled to avoid stress corrosion cracking.

There are many instances cited in the literature where residual stresses in combination with aggressive ions such as chlorides have caused cracking in austenitic stainless steels. In fact, more failures have been due to unaccounted residual stresses than the actual applied loads. For numerous applications using stainless steels, cold deformation is the final manufacturing operation. Any inhomogeneous deformation can result in residual stresses and such stresses, sometimes as high as the yield stress, could exist as a result of even a simple operation like straightening or bending. In large components where heat treatment is not possible, it is necessary to know to what extent cold work can be permitted without the risk of stress corrosion cracking. Khatak *et al* (1979) have carried out studies on the susceptibility of types 316 ss with different degrees of cold work, in boiling 45% $MgCl_2$ solution. Their results showed that cold working up to 15% reduction in thickness renders these steels susceptible to stress corrosion cracking. The maximum time for crack appearance was 10 hr for specimens without any external stress. For specimens with external stress, there was a further progressive decrease in cracking time with increase in cold work. Muraleedharan *et al* (1985) found that almost similar effects are seen in type 316 ss. For both steels at all stresses, SCC initiated in the transgranular mode. The fracture mode changed to intergranular in the case of 316 ss while in the case of type 304 ss transition from transgranular to intergranular mode occurred only in specimens that have been cold worked to very high levels (26 and 56%). There was a general tendency for an increase in the intergranular fracture area with increased level of cold work and applied stress. Bandyopadhyay *et al* (1981) investigated the stress corrosion

behaviour of welded specimens of cold worked type 316 ss and found that the welded specimens have a higher susceptibility to stress corrosion cracking.

Depending on the method of stressing test specimens, test procedures for stress corrosion cracking evaluation can be grouped into: (1) the constant load method, (2) the constant strain method, and (3) the slow dynamic straining method. Among these methods, the dynamic straining test has been the most favoured technique today because it is a severe test capable of producing cracking in a relatively short time with good reproducibility. However, there is scepticism about the use of the dynamic straining method for comparing the SCC susceptibility of similar alloys with different metallurgical/microstructural conditions and therefore having a wide difference in their ductilities. Khatak *et al* (1984) have evaluated the effect of cold rolling on the SCC propensity of type 316 ss using different test methods with a view to establishing the suitability of these methods, especially the dynamic straining method, by comparing the SCC resistance of materials having wide variations in their mechanical properties. These investigations showed that the use of parameters such as the ratio of UTS, ratio of total elongations and cracking index obtained through dynamic straining tests on such materials might give erroneous results and that crack growth rate could be a suitable criterion for evaluation of SCC susceptibility.

6. Estimation of secondary phases

When austenitic stainless steel and its weld metal are exposed to elevated temperatures during service, precipitation of various phases such as carbides, chi and sigma takes place. Relatively minor amounts of these phases can have major effects on the corrosion properties of the stainless steels. Therefore, a knowledge of the type, amount, and physical parameters of all phases is vital for the achievement of the optimum properties in stainless steels.

Some of the necessary information about the phases present can be obtained from microstructural analysis by physical methods like optical metallography, x-ray diffraction, electron microscopy and electron probe microanalysis. However, for a multi-phase alloy, it is also advantageous to know the precise distribution of elements between the different phases, the quantity of the individual phases and their lattice parameters. This is possible by separating the phases and consolidating them free of matrix contamination. The essential principle of separation of the phases is based on the selective dissolution of the matrix under appropriate conditions. Generally, the schemes of separation are based either on chemical and/or electrochemical techniques. The chemical reagents, like an alcoholic solution of bromine, are not always specific. The electrolytic anodic dissolution technique using electrolytes such as hydrochloric acid in a miscible organic solvent is widely used. This electrochemical technique is quantitative for the separation of the carbide phase but it is semi-quantitative for the separation of the delta-ferrite and sigma phases.

6.1 *Estimation of delta-ferrite*

The presence of delta-ferrite between 2 and 10% in the austenitic stainless steel welds is necessary to avoid the incidence of hot cracking. Techniques and standard procedures for measuring ferrite levels to the required accuracy are not available so

far. The magnetic (probe), x-ray diffraction, and metallographic methods make only surface or limited volume measurements. Schaeffler and DeLong diagrams can also be used for the measurement of delta-ferrite if the chemical composition of the weld deposit is known. But the accuracy of such a measurement is only 3 to 4%. The absolute content of delta-ferrite, however, can be determined by using an electrochemical technique (Gill *et al* 1979).

The technique consists of exposing a sample of the weld to an electrolyte (3·6 N H_2SO_4 containing 0·1 N NH_4SCN) at a fixed potential (−80 mV vs SCE) as shown in figure 11. At this critical potential, the austenite of the duplex austeno-ferrite microstructure is selectively dissolved while ferrite which becomes passive remains undissolved. The undissolved ferrite is then cleaned in a mixture of H_2SO_4 and HNO_3 and washed with methanol, dried and weighed.

The complete dissolution of austenite requires exposure of the sample for a long period, which depends on the thickness of the specimen and its ferrite content. During this long period some loss of ferrite is bound to occur. The error thus introduced can be eliminated if a correction factor is applied with respect to the loss of ferrite in its passive state. Calculation shows that maximum error introduced due to ferrite dissolution in this condition is only 1% of the estimated ferrite value.

This technique can also be used to study the following:

[a] The morphology of delta-ferrite after the austenite phase has been selectively dissolved from the duplex structure.
[b] The chemical composition of delta-ferrite.
[c] The decay kinetics of delta-ferrite during elevated temperature ageing in stainless steels (e.g. type 308) where other magnetic phases like martensite nucleate and interfere with the evaluation of ferrite content by magnetic methods.

6.2 *Estimation of other secondary phases*

While it is possible to individually separate various phases from the austenitic stainless steel matrix by careful adjustment of electrode potentials by a potentiostat,

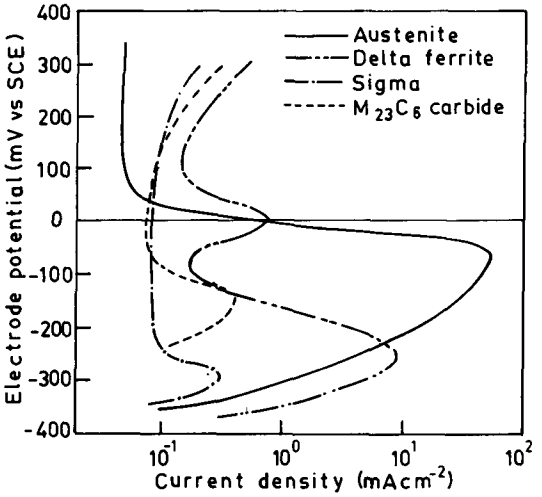

Figure 11. Anodic polarization curves in 3.6 N H_2SO_4 containing 0.1 N NH_4SCN.

a more convenient technique is to separate the secondary phases from the austenite by the electrochemical technique (as described for the separation of delta-ferrite) and then individually separate the phases by selective chemical dissolution, since preparation of the powders of the secondary phases into electrodes for electrochemical separation is a very involved and time consuming process.

A sample containing a mixture of secondary phases like delta-ferrite – $M_{23}C_6$, sigma – $M_{23}C_6$ or Chi – $M_{23}C_6$ dispersed in the austenite matrix can be analyzed for the estimation of individual phases by a combination of electrochemical and chemical techniques (Gill and Gnanamoorthy 1982). For chemically separating the phases, a 5% Br_2 – CH_3OH solution is employed. As shown in figure 12, the delta-ferrite and sigma phases dissolve rapidly in this solution and dissolution is complete in 50 and 70 minutes respectively. The complete dissolution of the Chi phase (not shown in the figure) takes about 40 minutes in this solution. But the dissolution rate of $M_{23}C_6$ is relatively slow. In 70 minutes, when the other secondary phases are dissolved completely, only about 1% $M_{23}C_6$ is dissolved. The weight fractions of various phases can then be calculated as shown in figure 13.

6.3 *Growth kinetics of secondary phases – application of phase separation techniques*

A number of samples were sectioned from type 316L stainless steel weld deposit and heat treated at 773, 873 and 973 K for durations ranging from 0·5 to 5000 hr. The electrochemical extraction of the precipitate was carried out as described earlier. The residue obtained from the electrochemical extraction process was analysed by X-ray diffraction using CuK_α radiation (Gill *et al* 1986b). In the as-deposited sample, only delta-ferrite was present, whereas samples aged at 773 K contained sigma, chi and $M_{23}C_6$ in addition to untransformed ferrite. However, the residue obtained from samples aged at 873 and 973 K contained sigma and $M_{23}C_6$.

The data for the total amount of extract obtained as a function of ageing time at different ageing temperatures are shown in figure 14. There is a general increase in

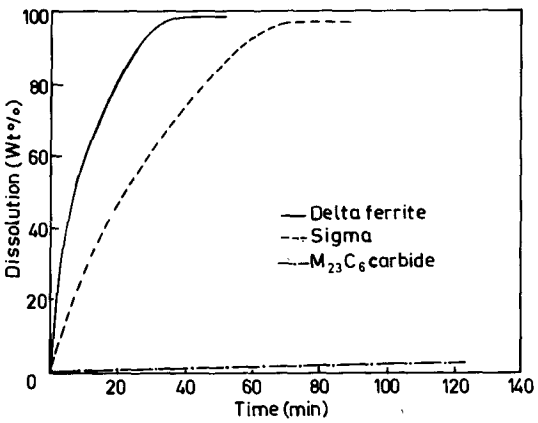

Figure 12. Dissolution behaviour of delta-ferrite, sigma and $M_{23}C_6$ in 5% Br_2-CH_3OH solution.

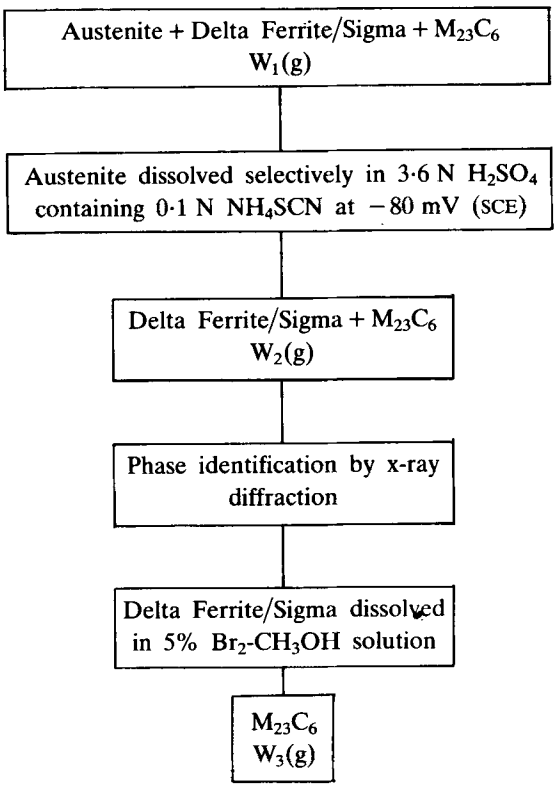

$$\text{Wt. \% delta-ferrite/sigma} = \frac{W_2 - W_3}{W_1} \times 100$$

$$\text{Wt. \% } M_{23}C_6 = \frac{W_3}{W_1} \times 100$$

Figure 13. A schematic plan of the electrochemical and chemical techniques for the separation and estimation of secondary phases in austenitic stainless steels.

the content of secondary phases with increasing temperatures. But the increase is higher as the temperature of ageing is raised.

The results for the chemical separation of $M_{23}C_6$ and sigma from the extracts obtained from the electrochemical extraction process are shown in figures 15 and 16 respectively. It is noted that the carbide grows rapidly at an ageing temperature of 773 K. However, at higher temperatures of ageing, the carbide growth is rapid during the initial stages of ageing but the dissolution process sets in on further ageing. The time of ageing needed to dissolve the carbide depends on the temperature of ageing. For example, an ageing time of 200 hr is needed at 873 K and about 20 hr at 973 K for the dissolution process to be predominant.

It is also interesting to note that the plateau regions observed in the growth kinetics of sigma (figure 16) correspond to the ageing times when $M_{23}C_6$ starts dissolving on further ageing. This indicates interdependence of the growth of sigma

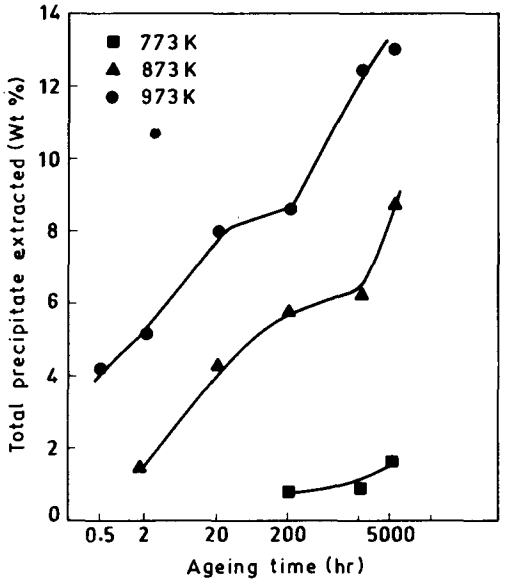

Figure 14. Total amount of precipitate extracted from the aged samples as a function of ageing time.

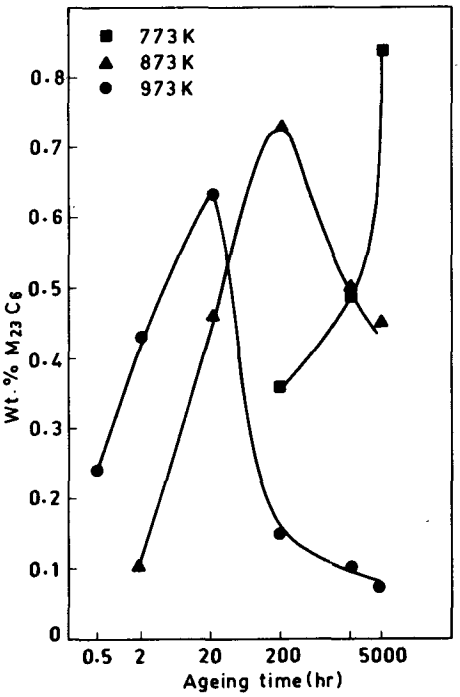

Figure 15. Amount of $M_{23}C_6$ formed during ageing as a function of ageing time.

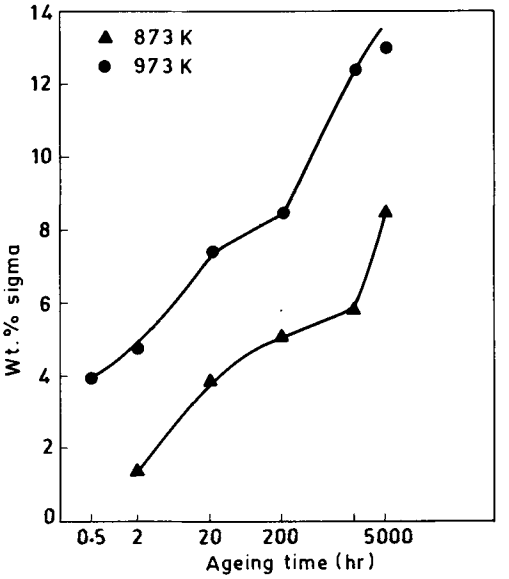

Figure 16. Amount of sigma formed as a function of ageing time.

and the dissolution of the carbides. The formation and resolution of $M_{23}C_6$ during thermal ageing has also been observed by other investigators using electron microscopy. However, the electrochemical and chemical methods of phase separation provide a method of studying this phenomenon quantitatively.

7. Conclusion

Most of the corrosion problems occurring in stainless steel structures and equipment can be prevented or minimised by (i) the proper choice of the construction material, welding electrodes and welding procedures, (ii) adopting scrupulous cleanliness during handling, and (iii) controlling the water chemistry of the environment at all stages of fabrication, storage and service.The optimum metallurgical condition of the material should be ensured so that it is free from sensitization or residual stresses. With these precautionary measures at the design and fabrication stages, the service-life of the austenitic stainless steel structures could be extended to very many years without costly shut-down and maintenance.

References

Bandyopadhyay G, Khatak H S, Mannan S L, Gnanamoorthy J B and Rodriguez P 1981 *Proc. workshop on experience in the fabrication and use of stainless steel equipment in DAE projects* (Kalpakkam: Reactor Research Centre) vol. **3** C-66

Dayal R K and Gnanamoorthy J B 1979 *Chem. Age India* **30** 483

Dayal R K and Gnanamoorthy J B 1980a *Corrosion (Houston)* **36** 104

Dayal R K and Gnanamoorthy J B 1980b *Corrosion (Houston)* **36** 433

Dayal R K and Gnanamoorthy J B 1982 *Trans. Indian Inst. Met.* **35** 43

Dayal R K and Gnanamoorthy J B 1983a *Br. Corros.* **18** 184

Dayal R K and Gnanamoorthy J B 1983b *Corros. Maintenance* **6** 301

Dayal R K and Gnanamoorthy J B 1984 *Proc. Ninth Int. Cong. Met. Corros* **3** 141

Dayal R K, Parvathavarthini N, Gnanamoorthy J B, Rodriguez P and Prasad Y V R K 1984 *Mater. Lett.* **2** 248

Dayal R K, Parvathavarthini N, Venkadesan S, Mannan S K and Gnanamoorthy J B 1981 *Proc. workshop on experience in the fabrication and use of stainless steel equipment in DAE projects* (Kalpakkam: Reactor Research Centre) vol. **3**, C-66

Dayal R K, Venkadesan S and Gnanamoorthy J B 1978 Reactor Research Centre, Kalpakkam, *Time-temperature sensitization diagrams for Virgo 14 Sb steel* Report No. RRC-35.

Gill T P S, Dayal R K and Gnanamoorthy J B 1979 *Welding Res. Suppl.* **58** 375-s

Gill T P S and Gnanamoorthy J B 1982 *J. Mater. Sci.* **17** 1513

Gill T P S, Gnanamoorthy J B and Padmanabhan K A 1986a *Corrosion* (in press)

Gill T P S, Vijayalakshmi M, Gnanamoorthy J B and Padmanabhan K A 1986b *Welding Res. Suppl.* **65** 122-s

Gnanamoorthy J B and Balachandra J 1973 *J. Electrochem. Soc. India* **22** 257

Kamachi Mudali U, Dayal R K, Gill T P S and Gnanamoorthy J B 1986 *Werkst. Korros.* (in press)

Khatak H S and Gnanamoorthy J B 1979 *Proc. Second Natl. Conf. on Corrosion and its control* (Karaikudi: SAEST) 1.6, p. 73

Khatak H S, Mannan S L, Gnanamoorthy J B and Rodriguez P 1979 *Chem. Age India* **30** 491

Khatak H S, Muraleedharan P, Gnanamoorthy J B, Rodriguez P and Padmanabhan K A 1984 *Proc. sixth international conference on fracture*, Poster papers, pp. 153

Muraleedharan P, Khatak H S, Gnanamoorthy J B and Rodriguez P 1985 *Metal. Trans.* **A16** 285